

Evolution of Cluster Galaxies in Hierarchical Clustering Universes

Takashi OKAMOTO and Asao HABE

*Division of Physics, Graduate School of Science, Hokkaido University, Sapporo 060-0810**E-mail(TO): okamoto@astro1.sci.hokudai.ac.jp*

(Received 1999 November 22; accepted 2000 February 14)

Abstract

Using cosmological N -body simulations of critical (SCDM) and open ($\Omega = 0.3$, OCDM) cold dark matter models, we investigated the evolution of cluster galaxies. Based on our numerical simulation, we constructed merging history trees of the galaxies. By following their merging history, we could show that the major merger fractions of the galaxies in cluster-forming regions is roughly proportional to $(1+z)^{4.5}$ at low redshifts ($z < 2$), and has a steep peak at $z \simeq 2.5$ and $z \simeq 3$ in SCDM and OCDM, respectively. We also show that the cluster galaxies are affected by the tidal interaction after the clusters are formed. Because the formation redshift of the cluster in SCDM, $z_{\text{form}} = 0.15$, is much more recent than that of the cluster in OCDM, $z_{\text{form}} = 1.6$, the cluster galaxies in SCDM show more rapid evolution by tidal interactions from $z = 0.5$ than those in OCDM.

Key words: galaxies: clusters: general — galaxies: general — galaxies: halos — galaxies: interactions

1. Introduction

Rich clusters of galaxies are large laboratories for studying galaxy evolution (Dressler 1984), and their evolution can be followed with samples out to $z \sim 1$ (Rosati et al. 1998). It is well established that galaxy populations vary with the density of neighboring galaxies in clusters of galaxies (Dressler 1980) and depend on the distance from the clusters' centers (Whitmore et al. 1993). The increase in the fraction of blue, star-forming cluster galaxies with the redshift (Butcher, Oemler 1978, 1984a, 1984b) has also been well established. It has been suggested that galaxy-galaxy and galaxy-cluster interactions play important roles in these effects; especially, a major merger of galaxies produces elliptical galaxies as merger remnants (Barnes 1989, 1996) and cumulative tidal interactions induce a morphological transformation of spiral galaxies to S0 galaxies.

Since it is generally believed that cold dark matter dominates the mass in the universe, we expect that the formation process of dark matter halos significantly affects the process of the formation and evolution of galaxies. In this paper, we discuss our high-resolution cosmological N -body simulations which trace the motion of the dark matter particles and can resolve the galaxy-sized dark halos within a high-density environment. We also consider when the above mentioned interactions (i.e., major mergers and tidal interactions) act on the evolution of the cluster galaxies during the formation and evolution of clusters in a hierarchical clustering universe.

We should consider the hydrodynamical processes of the baryonic components in order to follow the evolu-

tion of galaxies. However, hydrodynamical simulations, e.g., smoothed particle hydrodynamics (SPH) simulations, need much more CPU time than collisionless simulations. Thus, it is difficult to obtain a wide dynamical range with such simulations. Here, we restrict ourselves to follow the evolution of dark matter halos and to use the galaxy tracing method described by Okamoto and Habe (1999, hereafter Paper I) to obtain merging history trees of galaxies.

Recently, some authors have studied the evolution of the dark matter halos of the cluster galaxies in SCDM (Ghigna et al. 1998; Paper I). The epoch of the formation of a cluster of galaxies is very sensitive to the value of the cosmological density parameter, Ω_0 (Richstone et al. 1992). Since the evolution of clusters affects the evolution of galactic halos within the clusters (Paper I), it is interesting to compare the evolution of cluster galaxies in various cosmological models with different values of the density parameter. Here, we examine two cosmological models: one is the critical universe ($\Omega_0 = 1$), and the other is the open universe ($\Omega_0 = 0.3$). For both models we assume that the mass of the universe is dominated by cold dark matter (CDM).

The plan of this paper is as follows: Techniques and parameters of the N -body simulations and the method of creation of merging history trees of galaxies are described in section 2. Our results are presented in section 3 and discussed in section 4.

2. Simulation

2.1. The Simulation Data Set

Our simulations followed the evolution of a isolated spheres of a radius, R_{sim} , in both the standard CDM (SCDM) universe ($\Omega = 1$, $h \equiv H_0/100 \text{ km s}^{-1}\text{Mpc}^{-1} = 0.5$, $\sigma_8 = 0.67$) and the open CDM (OCDM) universe ($\Omega_0 = 0.3$, $h = 0.7$, $\sigma_8 = 1$). The normalisations were chosen to approximately match the observed cluster abundance. We imposed the constraint of the 3σ peak with an 8 Mpc Gaussian smoothed density field at the center of each simulation sphere in order to obtain a rich cluster (Hoffman, Ribak 1991). The simulations were performed using a parallel tree-code, which was used in Paper I. To obtain a sufficient resolution to follow the evolution of the galaxy-sized halos with a relatively small number of particles, we used the multi-mass N -body code (Navarro et al. 1997; Paper I). These initial conditions of our simulations were made as follows.

First, only long-wavelength components were used for the realization of the initial perturbation in the simulation sphere using $\sim 10^5$ particles; we then performed a simulation with these low-resolution particles. After this procedure, we tagged the particles which are inside a sphere of radius 3 Mpc centered on the cluster center at $z = 0$. Next, we went back to the initial time stage, and then divided each tagged particles into 64 high-resolution particles according to the density perturbation that is realized by including additional shorter wavelength components. As a result, the total number of the particles became $\sim 10^6$.

We then calculated again the dark matter evolution using high- and low-resolution particles from the new initial condition. Our analyses were operated only for the high-resolution particles. The mass of a high-resolution particle was $m \simeq 5.5 \times 10^8 h^{-1} M_\odot$, and its softening length, ϵ , was set to 5 kpc.

The overall parameters and mass of the clusters in both simulations at $z = 0$ are listed in table 1.

2.2. Creation of Merging History Trees of Galaxies

To create merging history trees of galaxies, we have to identify the galactic dark halos in the sea of dark matter. The identification of halos in such environments is a critical step (Bertshinger, Gelb 1991; Summers et al. 1995). The most widely used halo-finding algorithm, called the friends-of-friends (e.g., Devis et al. 1985), is not acceptable, because it cannot separate substructures inside of large halos. Since the DENMAX algorithm (Bertshinger & Gelb 1991) shows good performance, we used its offspring SKID (Governato et al. 1997).

This algorithm groups particles by moving them along the density gradient to the local density maximum. The density field and the density gradient are defined everywhere by smoothing each particle using the SPH-like method with the neighboring 64 particles. At a given red-

shift, only particles with local densities greater than one-third of the virial density at that epoch are moved to the local density maximum. This threshold roughly corresponds to the local density at the virial radius. The final step of the process is to remove all particles that are not gravitationally bound to their parent halos. Here, halos which contain more particles than a threshold number, n_{th} , are identified as galactic halos. Unless we explicitly state, $n_{\text{th}} = 30$ is adopted. This is a large enough number to inhibit the numerical evaporation of halos (Moore et al. 1996a).

The method to create the merging history tree is similar to that mentioned in Paper I; the details are as follows.

We identify galactic halos with a 0.5 Gyr time interval, which is restricted by the disk space of our computer. Since this time interval is shorter than the dynamical time-scale of the clusters and the fading time-scale of evidence of starburst in galaxies, it is sufficiently short to construct the merger trees to investigate the effect of the merging of galaxies and the tidal interactions.

The three most bound particles in each halo are tagged as tracers. We consider three cases to construct the merger tree of galaxies.

First, if a halo at t_{i+1} , where i is the number of a time stage, has two or more tracers that are contained in the same halo at t_i , then the halo at t_{i+1} is defined as a *next halo* of the halo at t_i . In this case, the halo at t_i is a *progenitor* of the halo at t_{i+1} .

Next, we consider the case that some halos at t_{i+1} have one of three tracers of a halo at t_i . The halo that has a tracer which is more bound in the halo at t_i is chosen as the next halo of the halo at t_{i+1} .

Finally, if none of three tracers of a halo at t_i are contained in any halos at the next time stage (t_i), we refer the particle which is the most bound tracer of the halo at t_i as a *stripped tracer*. We thus call both the halos and stripped tracers *galaxies* throughout this paper.

We construct the merging history trees of galaxies in this way. A halo which has more than two progenitors at former time stage is referred as a *merger*. It often happens that satellite galaxies pass through a central halo. Such cases should not be considered as merging. Hence, we check that the tracers of galaxies at t_{i-1} , which are contained in a merger at t_i are still in the same halo at t_{i+1} .

In order to estimate the mass of a stellar component of a galaxy, we assume that the mass of the stellar component is proportional to the sum of the masses of its all progenitors (hereafter we call this mass the *summed-up-mass*). Except for the case in which a large fraction of the stellar component of the galaxies have been stripped during the halo stripping, this assumption may be valid. We estimate the summed-up-mass of a galaxy as the sum of the summed-up-masses of its all progenitors at the previous time stage. For a newly forming halo which has

Table 1. Parameters of simulations.

MODEL	N_h	N_l	ϵ_h [kpc]	ϵ_l [kpc]	m_h [$h^{-1}M_\odot$]	m_l [$h^{-1}M_\odot$]	R_{sim} [Mpc]	M_{cluster} [$h^{-1}M_\odot$]
SCDM	958592	91911	5	50	5.4×10^8	3.45×10^{10}	30	4.65×10^{14}
OCDM	1186240	94396	5	50	5.5×10^8	3.5×10^{10}	32	5.53×10^{14}

Subscripts h and l indicate high-resolution and low-resolution particles, respectively.

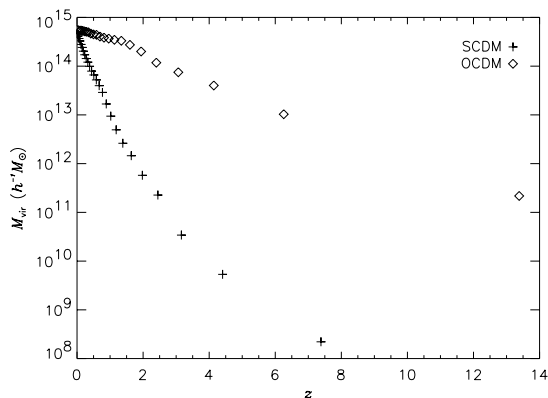


Fig. 1.. Mass evolution of the most massive virialized object in each model. The plus signs and diamonds represent the mass evolution of the SCDM cluster and the OCDM cluster, respectively.

no progenitors at a previous time stage, the summed-up-mass of the halo is set to the mass of the halo. To consider mass increase due to accretion of dark matter to the halo after its first identification, we replace the summed-up-mass with the halo mass when the summed-up-mass is smaller than the halo mass.

3. Results

3.1. Evolution of the Cluster

To define the size of clusters, we calculated the virial overdensity based on the spherical-collapse model. For the SCDM model we used 200 as the virial overdensity according to previous studies (e.g., Navarro et al. 1996). In OCDM, the virial overdensity is a function of redshifts. Therefore, we calculate it at each redshift and, it then became $\delta \simeq 400$ at $z = 0$. In figure 1, we plot the mass evolution of the most massive virialized object in each model. It is well known that the formation epoch of the OCDM cluster is much earlier than that of the SCDM cluster. In our result, the formation redshift (the redshift when the half of the final mass has accreted) of the SCDM cluster is $z \simeq 0.15$ and that of the OCDM cluster is $z \simeq 1.6$. We show the x - y projection of a density map in

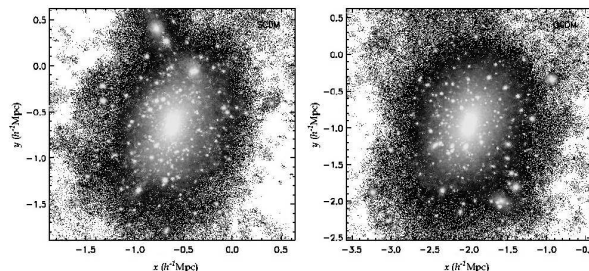


Fig. 2.. Density maps of the clusters at $z = 0$. The left panel represents the density map of the SCDM cluster and right panel represents that of the OCDM cluster.

a cube with sides of $2r_{\text{vir}}$ (r_{vir} is the radius of the sphere having the virial overdensity) centered on the cluster’s center in each model at $z = 0$ (figure 2). The gray scale represents logarithmic scaled density given by the SPH like method. We found that many galaxy-sized density peaks survive even in the central parts of the rich clusters.

3.2. Merging of Galaxies

Numerical simulations have shown that mergers with a mass ratio of 3:1 or less produce a remnant resembling an elliptical galaxy (Barnes 1996). Therefore, we define a halo which has more than two ancestors with this ratio at the former time stage as a “major merger.” In figure 3, we show the major merger fraction of the large galaxies ($10^{11}h^{-1}M_\odot \leq M_{\text{sum}} \leq 10^{13}h^{-1}M_\odot$) in the cluster-forming regions as a function of the redshift. The points in the figure can be fitted by a curve in Gottlöber et al. (1999), $\alpha(1+z)^\beta \exp[\gamma(1+z)]$, with $\alpha = 0.01, 0.04$, $\beta = 4.5, 4.6$, and $\gamma = -1.4, -1.2$ for SCDM and OCDM, respectively. When the clusters start forming, the merger fraction steeply decreases. One reason for this is that the high-velocity dispersion in clusters and groups inhibits the galaxies within these objects from merging with each other. Another reason is that the stripping of halos by tidal fields of such large objects prevents the merging of individual galactic halos (Funato et al. 1993; Bode et al. 1994). Since the cluster in OCDM forms much earlier than in SCDM (see figure 1), this de-

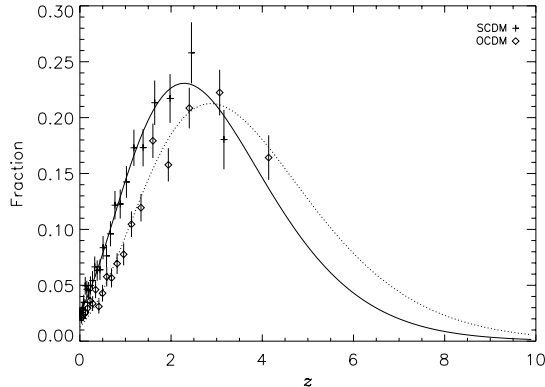


Fig. 3.. Major merger fractions of massive galaxies with $M_{\text{sum}} \geq 10^{11} h^{-1} M_{\odot}$ in cluster-forming regions. The plus signs and diamonds indicate the fraction in SCDM and in OCDM, respectively.

cline of the merger fraction appears at the higher redshift in OCDM than SCDM.

Governato et al. (1999) showed that the major merger rate of the galaxy-sized dark halos in the field for $z < 1$ is proportional to $(1+z)^{4.2}$ and $(1+z)^{2.5}$ in SCDM and OCDM, respectively. To compare their result obtained in the field to our result obtained in the cluster-forming regions, we can say that the efficiency of the major merging of galaxies in the cluster-forming regions more steeply increases toward high redshifts than in the field, especially in OCDM. Since the density contrast of the cluster-forming regions in OCDM takes a larger value than in SCDM, the evolution of major merger rate in OCDM is significantly different between in the field and in the cluster-forming regions.

Recently, van Dokkum et al. (1999) observed the rich cluster at $z = 0.83$, finding a high merger fraction in the cluster and rapid evolution of the fraction. The fraction in $z < 1$ is comparable to the result obtained here.

3.3. Tidal Stripping of Halos

We evaluated the effects of the tidal stripping on the galactic halos in different cosmologies. For this purpose, we chose galactic halos at a redshift when the number of large halos with $M_h \geq 10^{11} h^{-1} M_{\odot}$ is largest much before the cluster or group formation epochs. The tidal effects are probably negligible at such a redshift. Then, we examined whether the chosen galaxies lose their halos at lower redshifts. If they become $M_h < 10^{10} h^{-1} M_{\odot}$ at lower redshifts, they must be tidally stripped. We then adopted $n_{\text{th}} = 19, 18$ for SCDM and OCDM, respectively. Therefore, when a galaxy has become a stripped

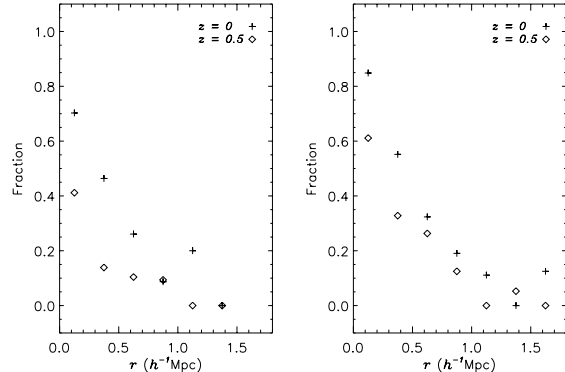


Fig. 4.. Stripped galaxy fractions of galaxies which have massive halos ($M_h \geq 10^{11} h^{-1} M_{\odot}$) at selected redshift in SCDM (left panel) and in OCDM (right panel). They are plotted in the $0.25 h^{-1}$ Mpc bins from each cluster center at $z = 0$ (plus signs) and at $z = 0.5$ (diamonds).

tracer, it means that the galaxy does not have a halo with $M_h \geq 10^{10} h^{-1} M_{\odot}$.

When they become such small halos, dissipative effects, which were not included in our simulations, should become important. We call such galaxies *stripped galaxies*.

In figure 4, we show the stripped galaxy fractions in the $0.25 h^{-1}$ Mpc radius bins from the cluster centers. The stripped galaxies show a similar distribution in both models at $z = 0$. Their evolutions, however, are very different between the models. In SCDM, there are few stripped galaxies, except for the central part at $z = 0.5$, and the fraction drastically increases near $z = 0$. On the other hand, we can see a strong correlation between the fraction and the radius in the OCDM cluster, even at $z = 0.5$; this fraction shows very weak evolution during $z = 0.5$ and 0. This is because the cluster in OCDM forms much earlier than in SCDM.

Next, we compared the radii of the halos, which were determined as the radii at which their circular velocity profiles take minimum values (Ghigna et al. 1998; Paper I), to the tidal radii of the halos estimated at their pericentric positions, which we calculated by using the dark halo model of Navarro et al. (1997). The tidal radii of the halos, r_{est} , were estimated by the following approximation assuming an isothermal distribution of dark matter:

$$r_{\text{est}} \simeq r_{\text{peri}} \frac{v_{\text{max}}}{V_c}, \quad (1)$$

where v_{max} is the maximum value of the circular velocity of a galactic halo and V_c is the circular velocity of a cluster. In figure 5, we plot r_{est} against r_h for the outgoing halos that must have passed pericenter recently. We

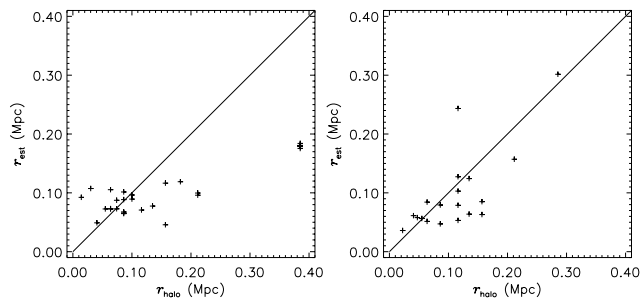


Fig. 5.. Measured values of the radii of the member halos against the expected values, assuming that the halos have isothermal mass distributions and are tidally stripped at their pericentric positions. Only out-going large halos are plotted. The left panel and right panel represent the halos in the SCDM cluster and those in the OCDM cluster, respectively.

plotted only the large halos ($v_c \geq 80 \text{ km s}^{-1}$) to avoid any influence of the insufficient resolution. Moreover, we ignored the halos with $r_{\text{peri}} < 300 \text{ kpc}$, because they have tidal tails due to impulsive collisions as they pass close to the cluster center (Ghigna et al. 1998; Paper I). In SCDM, most of the halos with $r_h > 100 \text{ kpc}$ have larger radii than r_{est} . On the other hand, the halos in OCDM are sufficiently truncated, and have comparable radii to r_{est} , because few galaxies accrete to the cluster in OCDM at low redshifts (the cluster has formed at $z_{\text{form}} = 1.6$). This means that the galaxies in the SCDM cluster tidally evolve, even at present, and such evolution has almost come to completion in the OCDM cluster. This result is consistent with the weak evolution of the stripped galaxy fraction of the cluster galaxies in OCDM.

4. Discussion

We have investigated the effects of the difference of the cosmological density parameter on the evolution of the cluster galaxies using the cosmological N -body simulations in SCDM and OCDM. The cluster forms at $z \simeq 0.15$ and $z \simeq 1.6$ in SCDM and OCDM, respectively. We have shown that the difference between the formation epochs of the clusters changes the evolution of the cluster galaxies.

The major merger fraction in the cluster-forming regions is roughly proportional to $(1+z)^{4.5}$ in each cosmological model at low redshifts ($0 < z < 2$). The decline of this fraction appears at higher redshifts in OCDM than in SCDM. The reason is as follows. The efficiency of merg-

ing rapidly decreases as clusters form because of large internal velocities of the clusters and a reduction of the size of tidally truncated halos. Hence, the earlier formation of the cluster in OCDM leads to an earlier decline of the major merger fraction. From this result, we expect that in a lower density universe the elliptical galaxies in clusters would mainly form earlier. We will investigate this possibility in a forthcoming paper.

The tidal interactions also have the possibility to change the morphology of the galaxies and to induce active star formation (Moore et al. 1996b, 1998). We find that, in the SCDM universe, the fraction of cluster galaxies which have been stripped of their dark halos due to tidal interactions begins to increase from $z \sim 0.5$. Thus, if the morphological transformation from S to S0 and the star burst due to the galaxy harassment (Moore et al. 1996b, 1998) are caused by such tidal interactions, the morphology-density relation and the Butcher–Oemler effect should evolve from $z \simeq 0.5$ in SCDM. On the other hand, in OCDM, since this fraction has already been significant at $z = 0.5$, we can observe these effects at higher redshifts than $z = 0.5$. For detailed analyses we need a star-formation history in each galaxy, which will be considered in future work.

In this paper we show how the cluster evolution affects on the evolution of cluster galaxies. The effects of different formation epochs of the clusters of galaxies between cosmological models on the color and morphological evolution of the cluster galaxies will be clarified by combining the merging history trees obtained here with a simple model of gas cooling, starformation, and feedback used in semianalytical work (Kauffmann et al. 1993; Cole et al. 1994; Kauffmann et al. 1999).

We wish to thank M. Fujimoto and M. Nagashima for useful discussions. Numerical computation in this work was carried on the HP Exemplar at the Yukawa Institute Computer Facility and on the SGI Origin 2000 at the Division of Physics, Graduate School of Science, Hokkaido University.

References

- Barnes J.E. 1989, *Nature* 338, 123
- Barnes J.E. 1996, in *Formation of the Galactic Halo, Inside and Out*, ed H. Morrison, A. Sarajedini ASP Conf. Ser. 92, p415
- Bertshinger E., Gelb J.M. 1991, *Comput. Phys.* 5, 164
- Bode P.W., Berrington R.C., Cohn H.N., Lugger P.M. 1994, *ApJ*, 433, 479
- Butcher H., Oemler A.Jr 1978, *ApJ* 219, 18
- Butcher H., Oemler A.Jr 1984a, *ApJ* 285, 426
- Butcher H.R., Oemler A.Jr 1984b, *Nature* 310, 31
- Cole S., Arag3n-Salamanca A., Frenk C.S., Navarro J.F., Zepf S.E. 1994, *MNRAS* 271 781

- Davis M., Efstathiou G., Frenk C.S., White S.D.M. 1985, ApJ 292, 371
- Dressler A. 1980, ApJ 236, 351
- Dressler A. 1984, ARA&A 22, 185
- Funato Y., Makino J., Ebisuzaki T. 1993, PASJ, 45, 289
- Ghigna S., Moore B., Governato F., Lake G., Quinn T., Sadel J. 1998, MNRAS, 300, 146
- Governato F., Moore B., Cen R., Stadel J., Lake G., Quinn T. 1997, NewAstron. 2, 91
- Gottlöber S., Klypin A., Kravtsov A.V. 1999, astro-ph/9909012
- Hoffman Y., Ribak E. 1991, ApJ 380, L5
- Kauffmann G., Colberg J.M., Deaferio, A., White S.D.M. 1999, MNRAS 303, 188
- Kauffmann G., White S.D.M., Guiderdoni B. 1993, MNRAS 264, 201
- Moore B., Katz N., Lake G. 1996a, ApJ 457, 455
- Moore B., Katz N., Lake G., Dressler A., Oemler A.Jr 1996b, Nature 379, 613
- Moore B., Lake G., Katz N. 1998, ApJ 495, 139
- Navarro J.F., Frenk C.S., White S.D.M. 1997, ApJ 490, 493
- Okamoto T., Habe A. 1999, ApJ 516, 591 (Paper I)
- Richstone D., Loeb A., Turner E.L. 1992, ApJ 393, 477
- Rosati P., Ceca R.D., Norman C., Giacconi R. 1998, ApJ 492, L21
- Summers F.J., Davis M., Evrard A.E. 1995, ApJ 454, 1
- van Dokkum P.G., Franx M., Fabricant D., Kelson D.D., Illingworth G.D. 1999, ApJ 520, L95
- Whitmore B.C., Gilmore D.M., Jones C. 1993, ApJ 407, 489